J|A|C|S
ARTICLES
Published on Web 03/18/2006

Synthesis of an Anionically Chargeable, High-Molar-Mass, Second-Generation Dendronized Polymer and the Observation of Branching by Scanning Force Microscopy

Edis Kasëmi,[§] Wei Zhuang,[‡] Jürgen P. Rabe,*[,‡] Karl Fischer,[⊥] Manfred Schmidt,[⊥] Martin Colussi,[§] Helmut Keul,[||] Ding Yi,[#] Helmut Cölfen,[#] and A. Dieter Schlüter*[,§]

Contribution from the Department of Materials, Institute of Polymers, Swiss Federal Institute of Technology, ETH-Hönggerberg, HCI J 541, 8093 Zürich, Switzerland, Department of Physics, Humboldt University Berlin, Newtonstrasse 15, D-12489 Berlin, Germany, Institute for Physical Chemistry, University of Mainz, Jakob-Welder-Weg 11, D-55099 Mainz, Germany, Institute for Technical and Macromolecular Chemistry, RWTH Aachen, Paulwelsstrasse 8, D-52056 Aachen, Germany, and Max Planck Institute of Colloids and Interfaces, Am Mühlenberg, D-14476 Golm-Potsdam, Germany

Received November 23, 2005; E-mail: rabe@physik.hu-berlin.de; dieter.schluter@mat.ethz.ch

Abstract: An efficient synthesis of a methacrylate-based, second-generation (G2) dendronized macromonomer and its free radical polymerization to the corresponding high-molar-mass G2 dendronized polymer are described. The molar mass is determined by gel permeation chromatography (GPC), light-scattering, and analytical ultracentrifugation and compared with values estimated from a scanning force microscopy (SFM) contour lengths analysis of individualized polymer strands on mica. The polymer carries terminal *tert*-butyl-protected carboxyl groups, the degree of deprotection of which with trifluoroacetic acid is quantified by NMR spectroscopy using the highest molar mass sample. SFM imaging of both protected (noncharged) and unprotected (charged) dendronized polymers on solid substrates reveals mostly linear chains but also some with main-chain branches. The nature of these branches is investigated and the degree roughly estimated to which they are formed. Finally, a synthetic model experiment is described which sheds some light on the aspect of whether chain transfer, a process that could lead to covalent branching, is of importance in the synthesis of the present dendronized polymers.

Introduction

Dendronized polymers are a class of comb polymers in which regularly branched units (dendrons) with a specific number of branching layers (generation numbers) are attached to a linear backbone at every repeat unit.[1] The higher the generation numbers are, the higher is the dendrons' space demand and, thus, the interaction between the tightly spaced (typically 2.5 Å) consecutive dendrons. This increased dendron/dendron interaction leads to an increased shape persistence which is a key difference between such macromolecules and those with the same backbone but without dendritic layer. The dendritic layer, however, not only impacts the shape persistence but also has the advantage that its thickness can be systematically varied by synthetic measures. Together with the ability of many dendronized polymers to be surface engineered,[2] these polymers exhibit interesting application options, which include to (a) pattern solid surfaces,[3] (b) move individualized macromolecules on solid substrates by use of a the scanning force microscope (SFM),[4] (c) do first steps toward a bottom-up approach to ordered functional arrays,[5] (d) apply a shielding concept to those representatives with fluorescent or electrically conducting backbones,[6] (e) let representatives substituted with mesogenic dendrons self-assemble into ordered bulk material,[7] and (f) let positively charged representatives self-assemble into huge ordered molecular aggregates.[8] Specifically the latter aspect, in which we see some future potential for the construction of hierarchically structured molecular objects of unprecedented dimensions, led the authors to develop dendronized polymers

[§] Swiss Federal Institute of Technology.
[‡] Humboldt University Berlin.
[⊥] University of Mainz.
[||] RWTH Aachen.
[#] Max Planck Institute of Colloids and Interfaces.

(1) Schlüter, A. D.; Rabe, J. P. *Angew. Chem., Int. Ed.* **2000**, *39*, 864−883. Zhang, A.; Shu, L.; Bo, Z.; Schlüter, A. D. *Macromol. Chem. Phys.* **2003**, *204*, 328−339. Frauenrath, H. *Prog. Polym. Sci.* **2005**, *30*, 325−384. Schlüter, A. D. *Top. Curr. Chem.* **2005**, *245*, 151−191.

(2) For example, see: (a) Ouali, N.; Méry, S.; Skoulios, A. *Macromolecules* **2000**, *33*, 6185−6193. (b) Grayson, S. M.; Fréchet, J. M. J. *Macromolecules* **2001**, *34*, 6542−6544. (c) Shu, L.; Gössl, I.; Rabe, J. P.; Schlüter, A. D. *Macromol. Chem. Phys.* **2002**, *203*, 2540−2550. (d) Suijkerbuijk, B. M. J. M.; Shu, L.; Klein Gebbink, R. J. M.; Schlüter, A. D.; van Koten, G. *Organometallics* **2003**, *22*, 4175−4177. (e) Zhang, A.; Barner, J.: Gössl, I.; Rabe, J. P.; Schlüter, A. D. *Angew. Chem., Int. Ed.* **2004**, *43*, 5185−5188.

(3) (a) Stocker, W.; Schürmann, B. L.; Rabe, J. P.; Förster, S.; Lindner, P.; Neubert, I.; Schlüter, A. D. *Adv. Mater.* **1998**, *10*, 793−797. (b) Percec, V.; Ahn, C.-H.; Ungar, G.; Yeardley, D. J. P.; Möller, M.; Sheiko, S. S. *Nature* **1998**, *39*, 161−164.

(4) Shu, L.; Schlüter, A. D.; Ecker, C.; Severin, N.; Rabe, J. P. *Angew. Chem., Int. Ed.* **2001**, *40*, 4666−4669.

(5) Barner, J.; Mallwitz, F.; Shu, L.; Schlüter, A. D.; J. P. Rabe, *Angew. Chem., Int. Ed.* **2003**, *42*, 1932−1935. Barner, J.; Al-Hellani, R.; Schlüter, A. D.; Rabe, J. P., submitted.

with such peripheral functional groups that can be turned into negatively charged ones. In this way, the already existing polyelectrolytes, based on dendronized polymers with hundreds or even thousands of positive peripheral charges per macromolecule, would have interesting counterparts to explore their individual and joint aggregation behavior.

This paper describes the synthesis of a G2 macromonomer with peripheral *tert*-butyl-protected carboxylates and a methacrylate polymerizing unit, as well as its free radical polymerization using azobisisobutyronitrile (AIBN) as initiator precursor. The molar masses of the corresponding G2 dendronized polymers were determined by three methods: gel permeation chromatography (GPC) using a calibration based on two-angle light-scattering and viscometry, static and dynamic multiangle light-scattering, and analytical ultracentrifugation. The obtained values were compared with those estimated on the basis of SFM contour lengths analysis. The SFM images of both protected and unprotected dendronized polymers on mica and polyornithine-coated mica exhibit primarily linear but also a trace amount of main-chain branched structures. Because branches had not been observed since the discovery of dendronized polymers some 10 years ago, their nature was investigated by a careful height analysis. This SFM work is complemented by a synthetic model study aiming at a quantification of an eventual covalent branching through chain-transfer events. Finally, the deprotection of the new G2 dendronized polymer will be described whereby the efficiency of this process was monitored by high-field NMR spectroscopy. For these experiments, the highest molar mass sample was used.

Results and Discussion

Synthesis. The synthetic steps are presented in Schemes 1−3. Macromonomer **6** uses the same main dendritic skeleton which proved successful in previous work.[9] It differs from this, however, by both the peripheral groups (*tert*-butyl-protected carboxylates instead of protected amines) and the polymerizable unit (acrylate instead of styrene). Its synthesis starts from the known G1 dendrons **1a** and **1c**.[10] Ester **1a** was reduced with LAH to give alcohol **1b**, which was then deprotected at its peripheral amines to furnish the ammonium chloride **2a**. Similarly, dendron **1c** was deprotected to **2b**, which was then reacted with the succinic acid mono *tert*-butyl ester **3** to yield the *tert*-butyl-protected carboxylate G1 unit **4a**. Its deprotection at the focal point to give **4b** was carried out according to the well-known Pd-catalyzed protocol for allylic esters.[11] G2 dendron **5** was then obtained by reacting an excess of **4b** with **2a** via standard peptide methods. Finally, macromonomer **6** was obtained by reacting this G2 dendron with freshly distilled methacrylic acid chloride. All neutral compounds were purified by column chromatography on silica gel and obtained as analytically pure, completely colorless materials. Monomer **6** was obtained on the 6 g scale as a foamy material. All structures were fully confirmed by NMR spectroscopic and mass spectrometric data.

Scheme 1 [a]

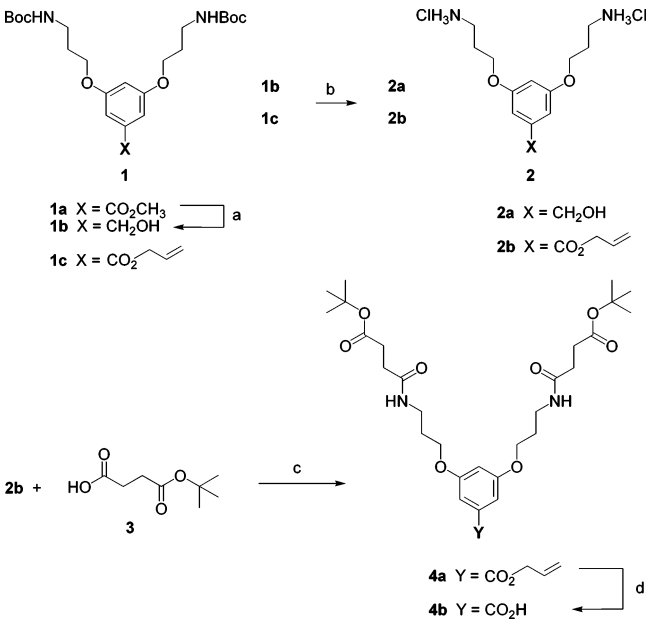

[a] Reagents and conditions: (a) **1a**, LAH, THF, 0 °C, 16 h (86%); (b) **1b**, **1c**, HCl/THF, rt, 6 h (95%); (c) HOBt, EDC, DCM, −20 °C, 16 h (76%); (d) **4a**, $Pd(PPh_3)_4$, $C_7H_7NaO_2S{\cdot}H_2O$, DCM/MeOH, rt, 4 h (80%).

The polymerizations were performed under nitrogen in highly concentrated DMF solution [2:1 (w/w) **6**:DMF; for example, 2.0 g of **6** in 1 mL of solvent] at 65 °C using 0.5−1.0 mol % of recrystallized AIBN. The initially clear and homogeneous solutions after 2−3 h showed a viscosity increase, and polymerization was continued for a further 8−10 h when the mixture had completely solidified. After three dissolution/precipitation cycles, polymer **7a** was obtained as a colorless, amorphous solid in 75−90% yield. Several experiments were performed, the conditions and results of which are collected in Tables 1 and 2. The molar mass data were obtained by GPC using a calibration based on two-angle light-scattering and viscometry, multiple-angle light-scattering, and analytical ultracentrifugation and were compared with those derived from SFM contour lengths analysis. (For a discussion, see the following section.)

The deprotection of dendronized polymer **7a** (Table 1, entry 5) to give **7b** was achieved with trifluoroacetic acid (TFA).[12] If a large excess of the acid per protecting group was applied at room temperature to the polymer in dichloromethane, a *tert*-butyl signal with a very small intensity compared to the original one of Boc remained in the ^{1}H NMR spectrum (see Supporting Information). If the deprotection was first done in neat TFA,

(6) For example, see: Bao, Z.; Amundson, K. R.; Lovinger, A. J. *Macromolecules* **1998**, *31*, 8647−8649. Sato, T.; Jiang, D.-L.; Aida, T. *J. Am. Chem. Soc.* **1999**, *121*, 10658−10659. Malenfant, P. R. L.; Fréchet, J. M. J. *Macromolecules* **2000**, *33*, 3634−3640. Jakubiak, R.; Bao, Z.; Rothberg, L. *Synth. Met.* **2000**, *61*, 114−118. Percec, V.; Obata, M.; Rudick, J. G.; De, M. Gloode, B. B.; Bera, T. K.; Magonov, S. N.; Balagurusamy, V. S. K.; Heiney, P. A. *J. Polym. Sci., Polym. Chem.* **2002**, *40*, 3509−3533. Pongantsch, A.; Wenzl, F. P.; List, E. J. W.; Leising, G.; Grimsdale, A. C.; Müllen, K. *Adv. Mater.* **2002**, *14*, 1061−1064.
(7) Kwon, Y. K.; Chvalun, S.; Schneider, A.-I.; Blackwell, J.; Percec, V.; Heck, J. A. *Macromolecules* **1994**, *27*, 6129−6132. Kwon, Y. K.; Chvalun, S.; Blackwell, J.; Percec, V.; Heck, J. A. *Macromolecules* **1995**, *28*, 1552−1558. Rapp, A.; Schnell, I.; Sebastiani, D.; Brown, S. P.; Percec, V.; Spiess, H. W. *J. Am. Chem. Soc.* **2003**, *125*, 13284−13297.
(8) (a) Gössl, I.; Shu, L.; Schlüter, A. D.; Rabe, J. P. *J. Am. Chem. Soc.* **2002**, *124*, 6860−6865. (b) Böttcher, C.; Schade, B.; Ecker, C.; Rabe, J. P.; Shu, L.; Schlüter, A. D. *Chem. Eur. J.* **2005**, *11*, 2923−2928.
(9) Neubert, I.; Schlüter, A. D. *Macromolecules* **1998**, *31*, 9372−9378.
(10) Ingerl, A.; Neubert, I.; Klopsch, R.; Schlüter, A. D. *Eur. J. Org. Chem.* **1998**, 2551−2556. Klopsch, R.; Koch, S.; Schlüter, A. D. *Eur. J. Org. Chem.* **1998**, 1275−1283. Zistler, A.; Koch, S.; Schlüter, A. D. *J. Chem. Soc., Perkin Trans. 1* **1999**, 501−508.
(11) Honda, M.; Morita, H.; Nagakura, I. *J. Org. Chem.* **1997**, *62*, 8932−8936.
(12) Girbasova, N.; Aseyev, V.; Saratovsky, S.; Moukhina, I.; Tenhu, H.; Bilibin, A. *Macromol. Chem. Phys.* **2003**, *204*, 2258−2264.

Scheme 2 [a]

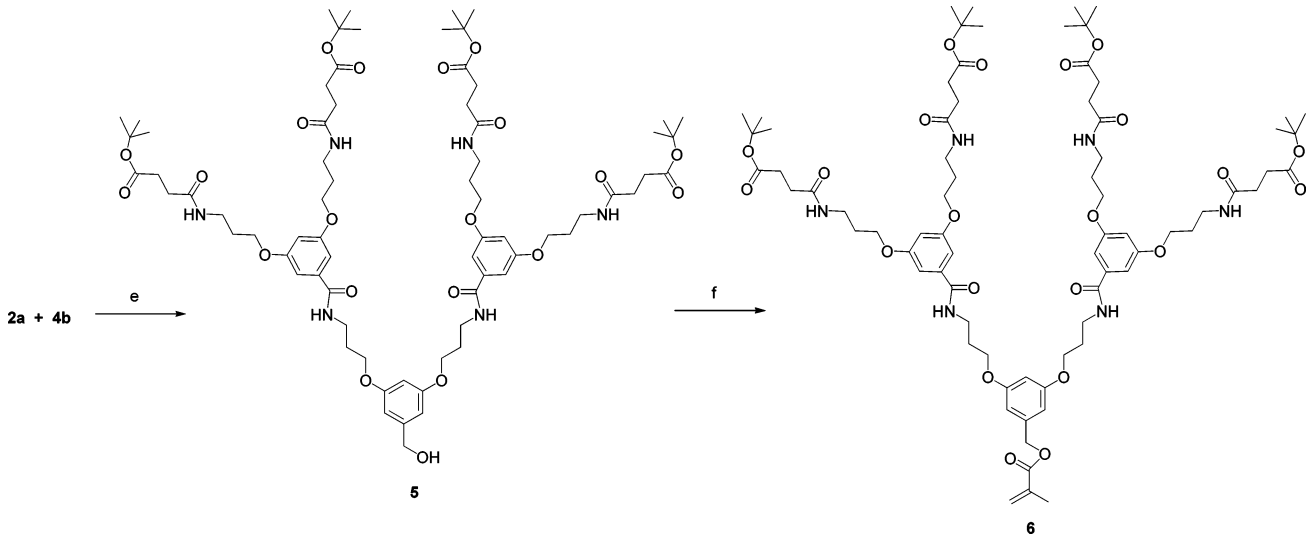

[a] Reagents and conditions: (e) HOBt, EDC, DCM, −20 °C, 16 h (60%); (f) MAC, DMAP, THF, rt, 16 h (85%).

Scheme 3 [a]

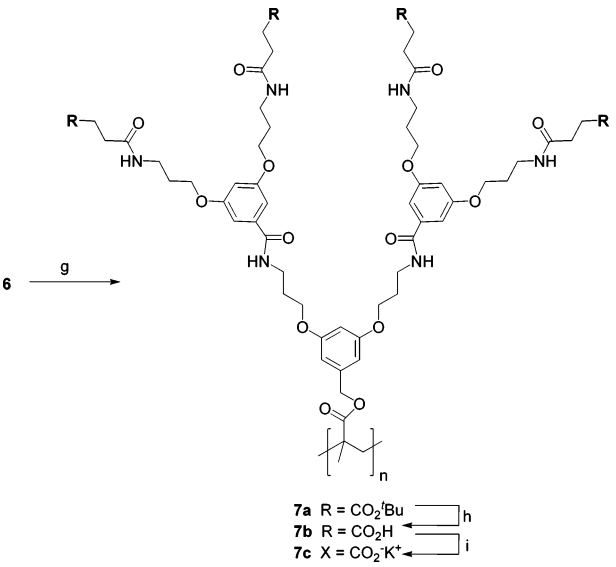

[a] Reagents and conditions: (g) AIBN, DMF, 65 °C, 12 h (90%); (h) TFA, rt, 24 h (95%); (i) KOH, MeOH, rt, 3 h.

followed by a second treatment in solution, even a highly amplified NMR spectrum did not show any indication of a *tert*-butyl signal anymore. It can be concluded that the deprotection is virtually quantitative. Given the molar mass of the sample of approximately $M_w = 7 \times 10^6$, approximately 20 000 esters per macromolecule were hydrolyzed. The deprotection procedure was not further optimized. The deprotonation of **7b**'s carboxylic acid functions to give the anionically charged polyelectrolyte **7c** was easily done with potassium hydroxide. Polymer **7c** was fully soluble in deionized water with pH = 8.5.

The glass transition temperatures of the polymers **7a**−**c** were determined by differential scanning calorimetry as 52 (**7a**), 53 (**7b**), and 125 °C (**7c**), respectively, on the basis of the second heating curves (see Supporting Information). Thermogravimetric analysis of **7a** under nitrogen indicated an abrupt and complete loss of the *tert*-butyl groups at 214 °C (see Supporting Information).

Molar Mass Determination by MALLS, AUC, and SFM Contour Lengths Analysis. (a) MALLS. The static and dynamic light-scattering results are summarized in Tables 1 and 2. The virial coefficients are positive, indicating that DMF is a good solvent for the G2 polymers. This is confirmed by the positive concentration dependence of the diffusion coefficients (see Supporting Information). Nonetheless, stiff polymers have the notorious tendency to form aggregates, a possible influence of which cannot be excluded for the present characterization, particularly for the light-scattering results. The Zimm plots of the two higher molar mass samples (see Supporting Information) do show a slight downward curvature at small q values which could be caused either by the broad molar mass distribution (i.e., by some extremely high molar mass chains) or by some aggregates. In our data analysis, this downward curvature was ignored; i.e., the molar masses and radii given in Tables 1 and 2 may be smaller than the true ones. It is also conceivable that some of the larger aggregated or nonaggregated chains are removed by filtration. However, such a concentration loss is assumed to be small and leads to smaller measured molar masses. Therefore, it is concluded that the molar masses represent a lower limit.

An inspection of the data given in Table 2 reveals that the reported radii do not fit the molar masses well; i.e., the data scatter significantly, which prohibits a more quantitative interpretation, e.g., in terms of chain stiffness.

(b) AUC. The molar mass of polymer **7a** (Table 1, entry 5) was also investigated by analytical ultracentrifugation. Sedimentation velocity experiments yielded the sedimentation coefficient distribution, together with the density distribution according to the procedure by Mächtle and Müller,[13] which is essentially based on the Schachmann density variation technique,[14] yielding a polymer density of 1.197 g/mL. It can be seen that the sedimentation coefficient distribution is broad (Figure 2), with the typical tailing toward higher molar masses,

(13) Mächtle, W. *Makromol. Chem.* **1984**, *185*, 1025−1039. Müller, H. G.; Herrmann, F. *Prog. Colloid Polym. Sci.* **1995**, *99*, 114−119.
(14) Edelstein, S. J.; Schachman, H. K. *J. Biol. Chem.* **1967**, *242*, 306−311.

Table 1. Conditions for and Results of the Radical Polymerization of Monomer **6** (Polymerization Time, 16 h)

entry	**7** (g)	DMF (μL)	AIBN (mol %)	yield (%)	M_n[a] ($\times 10^6$)	M_w[a] ($\times 10^6$)	PDI[a]	M_w[b] ($\times 10^6$)	M_w[c] ($\times 10^6$)	M_n[d] ($\times 10^6$)	M_w[d] ($\times 10^6$)
1	0.21	70	0.6	85	1.3	4.5	3.8				
2	0.23	80	0.8	78	1.3	3.3	1.8				
3	0.44	150	0.8	78	1.6	3.7	3.1	4.2			
4	1.00	450	1.0	87	2.6	7.8	2.9	5.8		1.1	3.1
5	2.22	1000	0.7	90	2.9	9.3	2.9	7.6	6.5	1.8	5.8

[a] GPC results calculated by light-scattering signals only. [b] MALLS in DMF without LiBr. [c] Analytical ultracentrifugation in NMP. [d] SFM contour length analysis.

Table 2. Summary of the Light-Scattering Results

entry[a]	M_w ($\times 10^6$ g mol^{-1})	R_g (nm)	R_h (nm)	A_2 ($\times 10^4$ cm^3 g^{-2} mol)
3	4.2	61	35	0.13
4	5.8	94	45	0.20
5	7.6	97	56	0.57

[a] The entry numbers refer to Table 1.

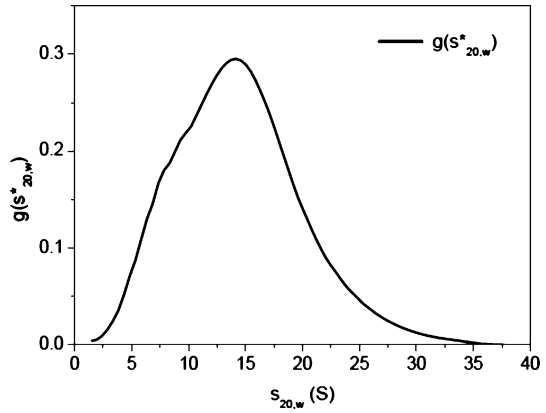

Figure 1. Differential sedimentation coefficient distribution, $g(s^*)$, vs sedimentation coefficient, s. The apparent sedimentation coefficients were corrected to their apparent standard values in water at 20 °C.

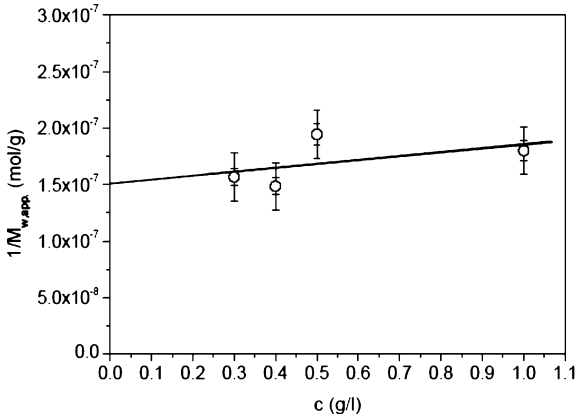

Figure 2. Plot of the inverse apparent weight-average molar mass, $1/M_{w,app}$, vs the concentration in NMP from sedimentation equilibrium for the extrapolation of M_w and the second osmotic virial coefficient A_2.

which can be expected for the applied synthesis conditions, consistent with the Schulz−Flory distribution. A slight bimodality is indicated for the part of the distribution with smaller sedimentation coefficients.

Sedimentation equilibrium experiments allowed for the determination of M_w and the second osmotic virial coefficient A_2 from an extrapolation of the inverse apparent weight-average molar mass $M_{w,app}$ to infinite dilution according to

$$\frac{1}{M_{w,app}} = \frac{1}{M_w} + 2A_2c$$

From this evaluation (Figure 2), a weight-average molar mass of 6.54×10^6 g/mol is calculated with a second osmotic virial coefficient of 1.69×10^{-5} cm^3·mol/g^2. The positive virial coefficient in *N*-methylpyrrolidone (NMP) indicates the absence of self-association and is a measure of nonideality. From it the excluded volume can be calculated to be 221 mL/g. This value is by a factor of 4 lower than the one from light-scattering, which can be attributed to the different applied solvents and also a slightly different molar mass (Tables 1 and 2).

(c) SFM Contour Length Analysis. Individualized dendronized polymer molecules (Table 1, entries 4 and 5) were spin-coated from dilute chloroform solutions (2−10 mg/L) onto freshly cleaved mica and visualized via tapping-mode SFM. The observed feature heights (apparent heights) were determined to be 1.6 nm (±10%), which is lower than the expected geometrical thickness, as typically observed in tapping-mode SFM of single macromolecules in air.[15] From their contour length distributions, the averages of their molar masses, M_n and M_w, were calculated assuming a length of the repeat unit of 0.25 nm (see Table 1).

The absolute values of both M_n and M_w for the samples of entries 4 and 5 of Table 1 are generally lower than those obtained by GPC, light-scattering, and ultracentrifugation. There are different possible reasons for this, one being that the backbone may not be in its *all-trans* conformation, which reduces the average length of the repeat unit to a value below 0.25 nm. Moreover, molecules were not counted for the contour analysis if they did not exhibit two clearly recognizable ends,[2c] e.g., if they aggregated intra- or intermolecularly. While the fraction of objects which could not be included in the statistical analysis is below approximately 10%, it is the very long molecules that are particularly prone to aggregate, thereby lowering the determined average molar masses. For linear brush polymers consisting of a long main chain with densely grafted linear side chains, several studies exist which compare the absolute molar mass as determined by scattering methods and the length of the polymers as determined by SFM.[16−20] The interpretation in terms of apparent length per main-chain repeat unit, l_m, on the surface gave strongly varying results, i.e., 0.07

(15) Zhuang, W.; Ecker, C.; Metselaar, G. A.; Rowan, A. E.; Nolte, R. J. M.; Samorí, P.; Rabe, J. P. *Macromolecules* **2005**, 38, 473−480 and references therein.
(16) Gerle, M.; Fischer, K.; Müller, A. H. E.; Schmidt, M.; Sheiko, S. S.; Prokhorova, S.; Möller, M. *Macromolecules* **1999**, *32*, 2629−2635.
(17) Börner, H. G.; Beers, K.; Matyjaszewski, K.; Sheiko, S. S.; Möller, M. *Macromolecules* **2001**, *34*, 4375−4383.
(18) Dziezok P.; Fischer, K.; Schmidt, M.; Sheiko, S.; Möller, M. *Angew. Chem., Int. Ed.* **1997**, *36*, 2812−2815.
(19) Li, C.; Gunari, N.; Fischer, K.; Janshoff, A.; Schmidt, M. *Angew. Chem.* **2004**, *116*, 1121−1124.
(20) Sun, F.; Sheiko, S. S.; Möller, M.; Beers, K.; Matyjaszewski, K. *J. Phys. Chem.* **2004**, *108*, 9682−9686.

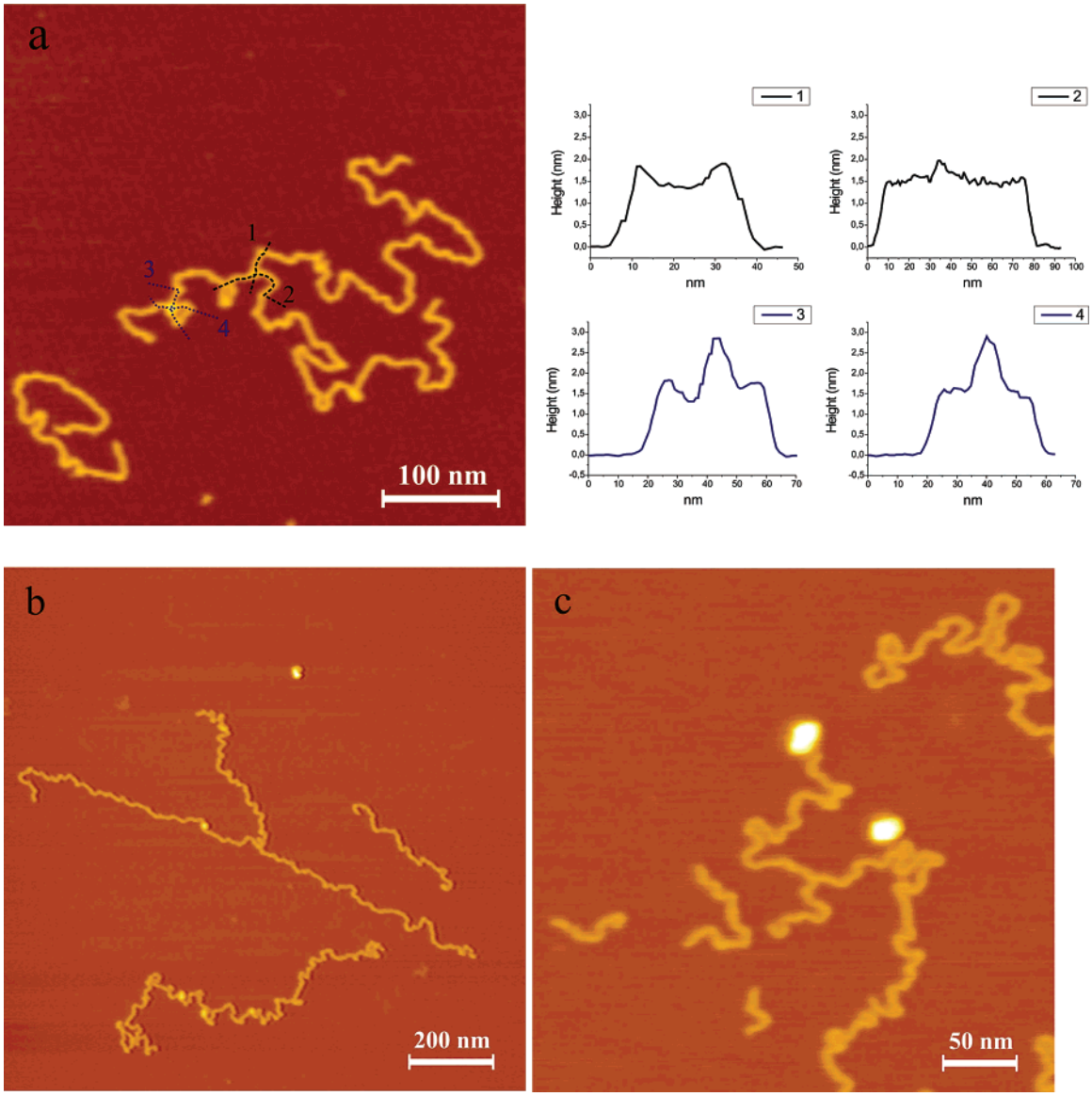

Figure 3. Tapping-mode SFM images of individualized protected, uncharged polymers (**7a**) on mica, some of which exhibit branches: samples of (a) entry 2, (b) entry 4, and (c) entry 5. The height traces along the contours in image a indicate chain crossing at the left and branching at the right junction. The white blobs on images b and c stem from unidentified material.

nm $< l_m <$ 0.23 nm, depending on side-chain length and grafting density, which are not always precisely known. The corresponding values for the dendronized polymers of entries 4 and 5 of Table 1 are $l_m = 0.13$ and $l_m = 0.19$, respectively. It should be noted that the reported light-scattering molar masses represent a lower limit, and accordingly the l_m values could become even smaller.

It seems that brush and dendronized polymers show a similar contraction behavior upon adsorption to solid substrates. The origin of this effect is not yet understood. Reports on l_m for cylindrical brush polymers in solution are contradictory.[16,21−27] The analysis of combined SLS/SANS data[28,29] has now provided some evidence that, irrespective of the side-chain lengths, the l_m values for cylindrical brushes are $l_m = 0.25$ and 0.23 nm in good and bad solvents, respectively. While many arguments exist as to why the conformation of the polymers at a surface in the dry state is different from that in solution, at least one example is reported where no difference was observed between cylindrical brush polymers in the dry state and adsorbed at a surface in the presence of solvent.[19]

By far most chains were linear; however, occasionally (on the order of 1% of all cases) main-chain branching was observed. Figure 3 displays three examples. While at crossing points of chains the thickness almost doubles, at the branches the height of the molecules does not vary significantly more than along the contours (Figure 3a). The accidental formation

(21) Fischer, K.; Gerle, M.; Schmidt, M. *Proc. ACS, PMSE Anaheim* **1999**, *30*, 133−134.
(22) Fischer, K.; Schmidt, M. *Macromol. Rapid Commun.* **2001**, *22*, 787−791.
(23) Terao, K.; Takeo, Y.; Tazaki, M.; Nakamura, Y. *Polym. J.* **1999**, *31*, 193−196.
(24) Terao, K.; Nakamura, Y.; Norisuye, T. *Macromolecules* **1999**, *32*, 711−716.
(25) Terao, K.; Hokajo, T.; Nakamura, Y.; Norisuye, T. *Macromolecules* **1999**, *32*, 3690−3694.
(26) Terao, K.; Hayashi, S.; Nakamura, Y.; Norisuye, T. *Polym. Bull.* **2000**, *44*, 309−316.
(27) Hokajo, T.; Terao, K.; Nakamura, Y.; Norisuye, T. *Polym. J.* **2001**, *33*, 481−485.
(28) Rathgeber, S.; Pakula, T.; Wilk, A.; Matyjaszewski, K.; Beers, K. L. *J. Chem. Phys.* **2005**, *122*, 124904-1−124904-12.
(29) Zhang, B.; Gröhn, F.; Pedersen, J. S.; Schmidt, M., in preparation.

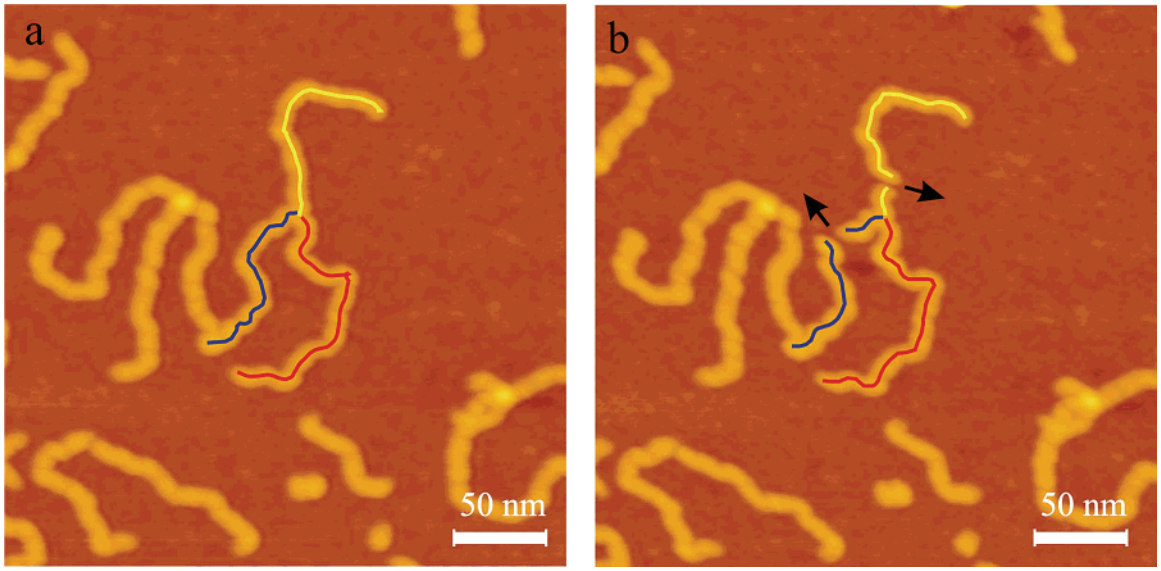

Figure 4. Tapping-mode SFM images of individualized unprotected, negatively charged polymers on polyornithine-coated mica before (a) and after (b) manipulation in contact mode. The three arms of a supposedly branched molecule are colored, and black arrows indicate the path the SFM tip followed during the manipulation attempts.

of T-like structures due to the adsorption of two different molecules meeting at one point is extremely unlikely. Provided there is no particular attractive interaction between a chain end and the main chain, this cannot explain the occurrence of about 1% of branched configurations in the diluted submonolayers investigated here.

We also considered whether it was possible to distinguish between covalently and noncovalently connected branches by exerting a force on the junction in order to estimate its strength.[5] However, while one can drag long dendronized polymers across a graphite surface using an SFM tip,[4] the same is not possible on mica, since the friction during manipulation on this substrate is so large that even short molecules break immediately. On the other hand, it was not possible to immobilize the molecules investigated here on graphite. We also tried to manipulate the deprotected, negatively charged polymers **7c** by spin-coating them from dilute aqueous solutions (5−10 mg/L) on a positively charged substrate, poly-L-ornithine-coated mica, which had been employed previously for the deposition of DNA.[8a] Figure 4 displays SFM images before and after manipulation, indicating that also in this case the interaction with the substrate is too strong to drag a long chain across the surface without breaking it immediately.

Experiment Regarding Chain Transfer. Chain transfer is one of the ways through which branch formation can occur during polymerization.[30] An active (radical) chain end abstracts, e.g., a hydrogen atom from its own or another independent chain,[31] with formation of an inactive chain end and a new radical center. If this is active enough to carry on polymerization, this leads to main-chain branching, and the radical's position marks the branch point. Supposed branching through chain transfer plays a role in the synthesis of dendronized polymer **7a**, and given the steric crowding around its backbone, hydrogen abstraction is considered more likely to take place at the dendritic shell rather than at the backbone. Preferred positions for the abstraction would be the CH bonds α to the ether oxygen atoms, the *tert*-butyl ester groups, or the benzylic groups. These bonds have lower dissociation energies than normal CH's.[32] To complement the above SFM findings from the synthetic side, an experiment was devised to prove or disprove the occurrence of chain transfer. Methyl methacrylate (MMA) was polymerized in the presence of a large amount of the third-generation (G3) dendron **8** (Figure 5) under conditions similar to the ones applied for macromonomer **6** (for details, see Supporting Information). This dendron has the same repeat units and protecting groups as the ones in macromonomer **6** and dendronized polymer **7a** and, thus, was considered an ideal compound to provoke chain transfer during the MMA polymerization. If it acted as a chain-transfer agent, formation of a PMMA was to be expected which carries this very dendron as an end group. In two independent experiments A and B, PMMAs with molar masses of M_w = 65 000 (A) and 450 000 g/mol (B) were obtained. The strongly amplified aromatic regions of the ^{1}H NMR spectra of these samples are compared (Figure 6a,b) with that of dendron **8** (Figure 6c) to evaluate potential dendron incorporation. The fact that there is no indication of dendron-typical signals in the PMMAs is a strong indication that, within the sensitivity of the NMR experiment, dendron **8** does not serve as a chain-transfer agent.[33] Spectra b and c of Figure 6 contain signals which cannot be associated with parent PMMA. To see whether they are somehow related to dendron **8** present in the polymerization mixture, MMA was also polymerized under the exact same conditions but without any dendron present. The NMR spectrum of the corresponding PMMA is shown in Figure 6d. As can be seen, most of the signals of unclear origin also appear there[34] and, therefore, cannot have anything to do with chain transfer by the dendron. Since the remaining signals' intensities by comparison with the ^{13}C satellites of the main PMMA signals

(30) Odian, G. *Principles of Polymerization*; Wiley: New York, 1991; pp 255−259.
(31) Chain transfer to solvent, monomer, radical initiator precursor, and alike is not considered here.
(32) McMillan, D. F.; Golden, D. M. *Annu. Rev. Phys. Chem.* **1982**, *33*, 493−532.
(33) This holds true at least as far as no decomposition of the dendron during chain transfer occurs.
(34) The differences in chemical shifts are assumed to be due to the different solvents used.

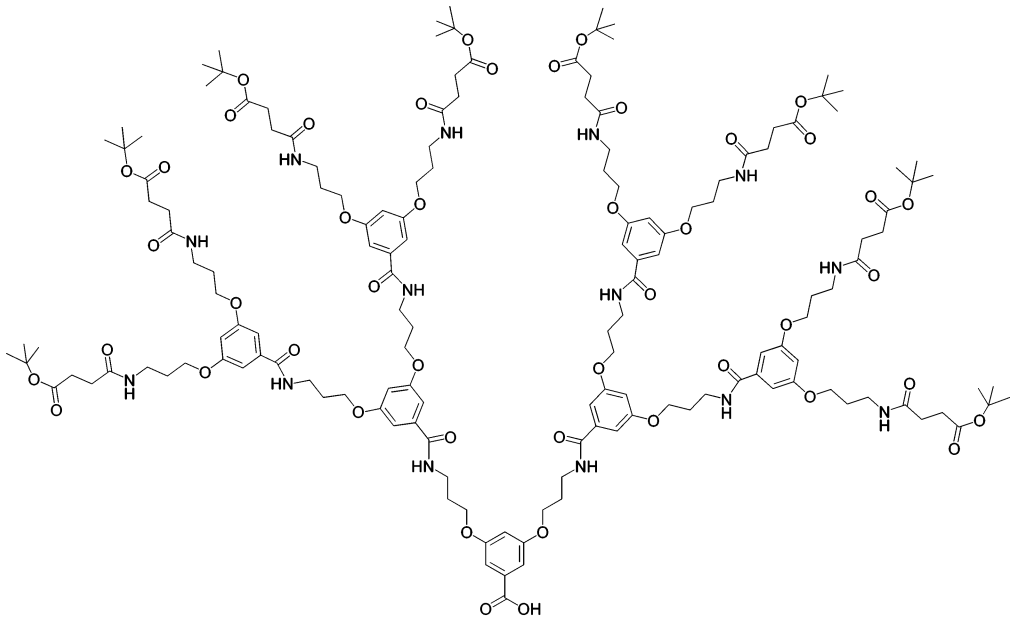

8

Figure 5. Chemical structure of the G3 dendron **8** used to provoke chain transfer.

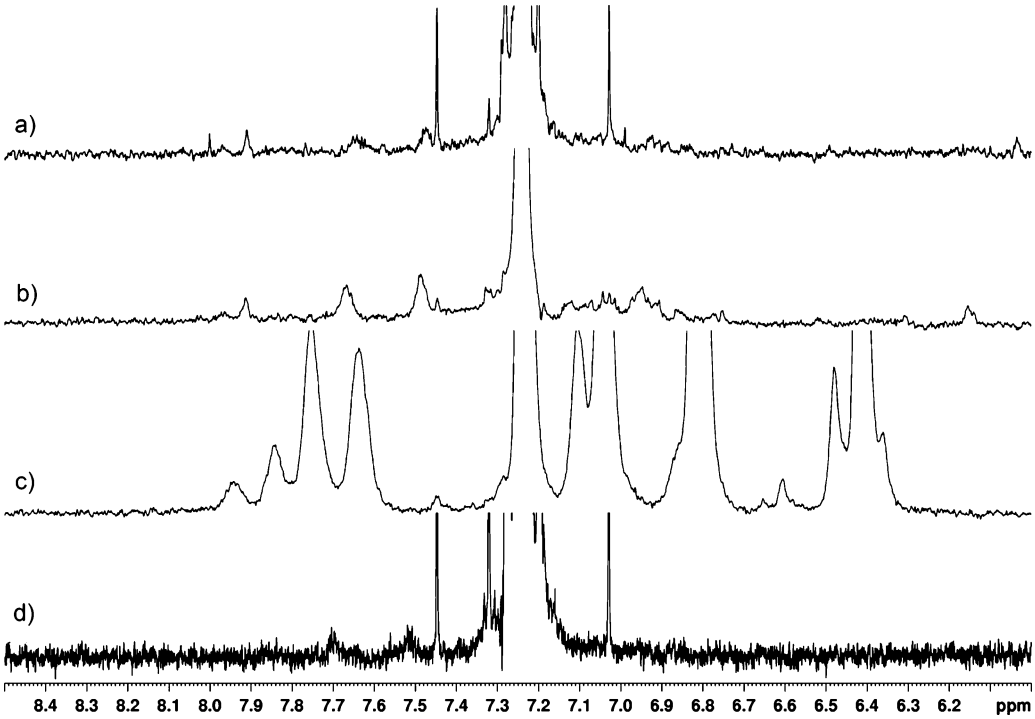

Figure 6. Highly amplified ^{1}H NMR spectra of two independent preparations of PMMA (M_w = 450 000 and 5000 g/mol, respectively) synthesized in the presence of G3 dendron **8** as a potential chain-transfer agent (a,b), the G3 dendron **8** (c), and a PMMA obtained under the same conditions but without any **8** present (d). The chloroform signal appears at $\delta = 7.25$; its ^{13}C satellites can be seen in spectra a and d.

(not shown) are in the sub-percent range, their significance was considered too low to be further investigated.

This model study supports the estimation based on SFM measurements that branching takes place in the sub-1% range. An eventual argument that a significant amount of branched structures may be contained in the approximately 10% of unidentifiable aggregates observed by SFM can be ruled out. It should also be noted that the branches do not seem to form exclusively by a gel effect at high conversion. A recent study using a G3 macromonomer based on dendron **8** (not described here) showed that branches also occur (in the sub-% range) at low conversions (e.g. 13%),

Conclusion and Outlook

The free radical polymerization of macromonomer **6** gave the G2 denpol **7a**, whose molar mass (M_w) was determined by several methods to be 8.5×10^6 (GPC), 7.6×10^6 (MALLS), 6.5×10^6 (AUC), and 5.8×10^6 (SFM). These values correspond to the highest chain lengths ever observed for a G2

dendronized polymer,[35] which indicates that it may be possible to also achieve longer chains for the corresponding G3 and G4 macromonomers than previously observed in related systems.[35a] If this is true, the key disadvantage of the macromonomer route to dendronized polymers could be overcome, which is that for high generations (G4) only relatively short chains have been so far accessible. Polymer **7a** was prepared on the 2 g scale. Deprotection of its approximately 20 000 *tert*-butyl ester groups to give **7c** was achieved under acidic conditions, and its degree was determined by high-field ^{1}H NMR spectroscopy to be virtually quantitative. Even under extreme amplification, no residual *tert*-butyl signal could be seen. The dendritic layer around the backbone stays intact under the deprotection conditions.

Given the respective limitations of the methods used, the molar mass values for polymer **7a** (Table 1, entry 5) match reasonably well. SFM has been used to observe branching of polymer chains, which occurs in the present systems at a concentration of approximately 1% only. Presently there is no other method available with this kind of sensitivity and the potential for positional identification of both the branching site and lengths of branches. The charged dendronized polymers will now be used to study their aggregation behavior, aiming at hierarchically structured three-dimensional matter.

Experimental Section

General. Compounds **1a**,[9] **1c**,[9] and **2b**[10] as well as the G3 dendron **8**[36] were synthesized according to literature methods. Other reagents were purchased from Aldrich, Across, or Fluka. Methacryloyl chloride (MAC) was freshly distilled before use. Tetrahydrofuran (THF) and triethylamine (TEA) were refluxed over Na with benzophenone as indicator. Dichloromethane (DCM) was dried by distilling over CaH_2. All other reagents and solvents were used as received. All reactions were performed under nitrogen atmosphere. Silica gel 60 M (Macherey-Nagel, 0.04−0.063 mm/ 230−400 mesh) was used as the stationary phase for column chromatography. Whenever possible, reactions were monitored by thin-layer chromatography (TLC) using TLC silica gel coated aluminum plates $60F_{254}$ (Merck). Compounds were detected by UV light (254 or 366 nm) and/or by treatment with a solution of ninhydrin in ethanol followed by heating. If not otherwise noted, ^{1}H and ^{13}C NMR spectra were recorded on Bruker AM 300 (^{1}H, 300 MHz; ^{13}C, 75 MHz) and AV 500 (^{1}H, 500 MHz; ^{13}C, 125 MHz) spectrometers at room temperature using chloroform-*d* as a solvent. High-resolution mass spectral (HRMS) and ESI-MS analyses were performed by the MS service of the Laboratorium für Organische Chemie at ETH Zürich. ESI-MS and MALDI-MS were run on an IonSpec Ultra instrument. In the case of MALDI-MS, 2,5-dihydroxybenzoic acid (DHB), 2-[(2*E*)-(4-*tert*-butylphenyl)-2-methylprop-2-enylidene]malononitrile (DCTB), or 3-hydroxypyridine-2-carboxylic acid (3-HPA) served as the matrix. The FAB experiments were carried out with 3-nitrobenzyl alcohol (MNBA)/CH_2Cl_2. Elemental analyses were performed by the Mikrolabor of the Laboratorium für Organische Chemie, ETH Zürich. The samples were dried rigorously under vacuum prior to analysis to remove strongly adhering solvent molecules. GPC measurements were carried out using a PL-GPC 220 instrument with a 2x PL-Gel Mix-B LS column set equipped with refractive index, viscosity, and light-scattering (with 15° and 90° angle) detectors (DMF + 1 g L^{-1} LiBr as eluent at 80 °C). Universal calibration was done using PMMA standards in a range of M_p = 2 680−3 900 000 (Polymer Labs Ltd., UK).

High-resolution thermogravimetric analysis (TGA) was performed on a Q500 thermogravimetric analyzer (TA Instruments, New Castle, DE). All measurements were carried out in an air stream under the same conditions. The mass loss with increasing temperature and its first derivative (DTG), which represents the change in decomposition rate, were plotted. Differential scanning calorimetry (DSC) was carried out under nitrogen at a heating or cooling rate of 10 °C/min on a DSC 7 instrument (Perkin-Elmer, Norwalk, CT). Two heating runs and one cooling run were consecutively carried out in a cycle, and the peak maxima were considered as the transition temperatures.

MALLS. Static and dynamic light-scattering measurements were performed with an ALV-SP86 goniometer, a Uniphase HeNe laser (25 mW output power at 632.8 nm wavelength), an ALV/High QE APD avalanche diode fiber optic detection system, and an ALV-3000 correlator. The static scattering intensities were analyzed according to mean square radius of gyration, $R_g^2 = \langle R_g^2 \rangle_z$, and the second virial coefficient A_2. The correlation functions showed a broad but monomodal decay and were fitted by a sum of two exponentials, from which the first cumulant Γ was calculated. The *z*-average diffusion coefficient D_z was obtained by extrapolation of Γ/q^2 to $q = 0$ and to infinite dilution. The inverse *z*-average hydrodynamic radius, $R_h = \langle 1/R_h \rangle_z^{-1}$, was evaluated by formal application of Stokes law. The dilute polymer solutions in DMF (typically 4−5 concentrations $0.05 \le c \le 0.5$ g/L) were measured from 30° to 150° in steps of 5° (SLS) or in steps of 10° (DLS). Prior to measurement, the solutions were filtered through 0.2 μm pore size Dimex filters (Millipore LG).

The refractive index increment was measured by a home-built Michelson interferometer as described elsewhere[37] and determined to be $dn/dc = 0.0962$ cm^3/g in DMF.

Analytical Ultracentrifugation. Sedimentation experiments were performed on an Optima XL-I instrument (Beckman Coulter, Palo Alto, CA) at 25 °C in cells with 12 mm 2.5° titanium center pieces (Nanolytics GmbH, Dallgow, Germany). For all experiments, the Rayleigh interference optics was applied. For the sedimentation equilibrium experiments, NMP was used as the solvent and the centrifugal speed was 3000 rpm. The sedimentation velocity experiments were performed in NMP (30 000 rpm) and DMF, the latter in the protonated (30 000 rpm as well as the deuterated form (20 000 rpm). For the determination of the sedimentation coefficient distribution simultaneously with the density distribution of the polymer, sedimentation velocity data in DMF and DMF-d_7 were combined following an algorithm published for latexes by Mächtle and Müller et al.[13] For the polymer density, the value at the maximum of the distribution was taken to be 1.197 g/mL (partial specific volume $\bar{v} = 0.835$ mL/g). Sedimentation equilibrium experiments were evaluated using the MSTAR algorithm,[38] and the weight-average apparent molar masses were extrapolated to infinite dilution to yield M_w as well as the second osmotic virial coefficient and excluded volume.

Scanning Force Microscopy. SFM images were recorded using a MultiMode scanning probe microscope (Digital Instruments, Inc., Santa Barbara, CA) operated in tapping mode. Olympus etched silicon cantilevers were used with a typical resonance frequency in the range of 200−400 kHz and a spring constant around 42 N/m. All samples were investigated at room temperature in air environment. As substrates we used freshly cleaved mica (PLANO W. Plannet GmbH, Wetzlar, Germany) or poly-L-ornithine (molar mass 30 000−70 000 g/mol, Sigma, St. Louis, MO)-coated mica. Contour lengths were determined taking into account the tip broadening, assuming a tip radius of 15 nm.

(35) For other high-molar-mass cases, see: (a) Zhang, A.; Zhang, B.; Wächtersbach, E.; Schmidt, M.; Schlüter, A. D. *Chem. Eur. J.* **2003**, *9*, 6083−6092. (b) Percec, V.; Ahn, C.-H.; Cho W.-D.; Jamieson, A. M.; Kim J.; Leman, T.; Schmidt, M.; Gerle, M.; Möller, M.; Prokhorova, S. A.; Sheiko, S. S.; Cheng, S. Z. D.; Zhang, A.; Ungar, G.; Yeardley D. J. P. *J. Am. Chem. Soc.* **1998**, *120*, 8619−8631.

(36) Kasëmi, E.; Schlüter, A. D., in preparation.

(37) Becker, A.; Köhler, W.; Müller, B. *Ber. Bunsenges.* **1995**, *89*, 600−605.

(38) Cölfen, H.; Harding, S. E. *Eur. Biophys. J.* **1997**, 25, 333−346.

Acknowledgment. This work was supported by the Deutsche Forschungsgemeinschaft (Sfb 448, TP A1 and A11), which is gratefully acknowledged.

Supporting Information Available: All synthetic procedures and analytical data, DSC and TGA curves of **7a**−**c**, ^{1}H and ^{13}C NMR spectra of **6**, ^{1}H NMR spectra of **7a**'s deprotection, GPC elution curve of **7a** (Table 1, entry 5), and Zimm plots. This material is available free of charge via the Internet at http://pubs.acs.org.

JA057964G